Electronic Supplementary Material (ESI) for Soft Matter.

Supplementary Material

Calculation of filament length:

Filament length was extracted from Eq.(2),

$$(2)\quad \frac{\eta_{eff}}{\eta_0} = A\left(\frac{L}{D}\right)^2 + 1 \quad ; \quad A = \frac{3}{4}\frac{\varphi}{\ln(1/\varphi)}\left(1 - \frac{\ln(\ln(1/\varphi))}{\ln(1/\varphi)} + \frac{0.6634}{\ln(1/\varphi)}\right) .$$

Since the filaments are double helical rigid rods, we assumed that the expression for their length is:

$$L = \frac{2}{3}\cdot\frac{d\cdot N_m}{nuc} ,$$

where d is the actin monomer diameter, N_m is the number of polymerized monomers, and nuc is the number of stable nuclei which we assumed do not change during the polymerization process.

φ is related to N_m by: $\varphi = \frac{V_m \cdot N_m}{V_{tot}}$, where V_m is the volume of G-actin monomer and V_{tot} is the total volume of the sample. Then, L and φ could be related through N_m and plugged into Eq.(2):

$$\frac{\eta_{eff}}{\eta_0} = \alpha\frac{\varphi^3}{\ln(1/\varphi)\cdot nuc^2}\left(1 - \frac{\ln(\ln(1/\varphi))}{\ln(1/\varphi)} + \frac{0.6634}{\ln(1/\varphi)}\right) + 1 \; ; \; \alpha = \frac{16}{27}\left(\frac{d\cdot V_{tot}}{D\cdot V_m}\right)^2 .$$

In order to find the parameter "nuc" for each initial actin monomer concentration, we used the known φ at the end of the polymerization process (where all the available monomers were polymerized), and the corresponding ratio $\frac{\eta_{eff}}{\eta_0}$ obtained from the experiment.

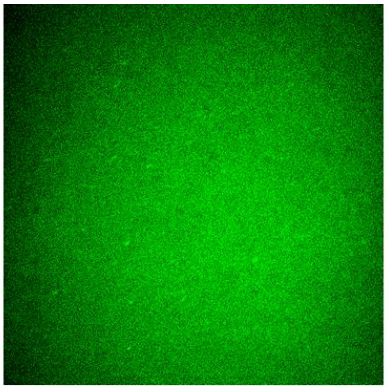

Fig. S1 Fluorescence image of an entangled stained with a fluorescent dye actin network, with initial monomer concentration of $c_A = 24\ \mu M$. Stained actin filaments cannot be resolved optically at this concentration.

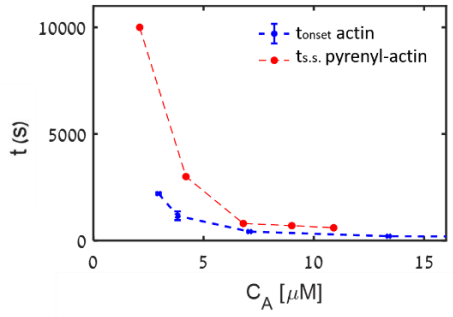

Fig. S2 Comparison between the effect of actin concentration on the time it takes a network to form, t_{onset}, and the time it takes a pyrenyl-actin to polymerize and reach a steady-state, $t_{s.s.}$ according to ref. [27]. The pyrene assay measurements represent the upper limit for the network formation time obtained in our method.

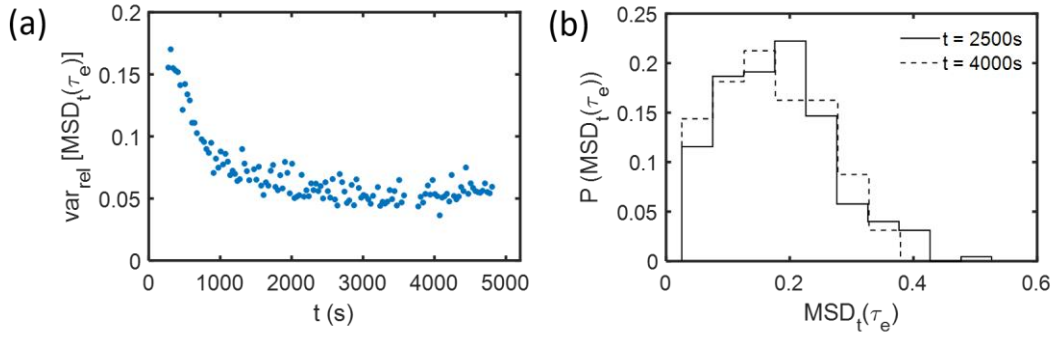

Fig. S3 The temporal evolution of the structural heterogeneity of entangled actin network with initial monomer concentration of $c_A = 4\ \mu M$. (a) The relative variance (var/mean) of the time averaged MSD of a single particle at lag time $\tau_e = 1/\omega_e$, (b) Probability distribution of the single particle time averaged MSD with a lag time of τ_e at t = 2500 s and 4000 s of the self-assembly process. The heterogeneity decreases during the first 2500 s of the polymerization process. At the relaxation period (i.e. 2500 s < t < 4000 s), no significant change in heterogeneity is observed.

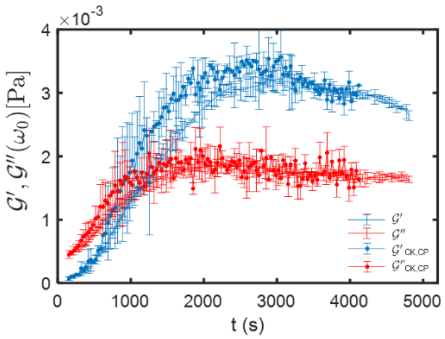

Fig. S4 Time evolution of $\mathcal{G}'(\omega_0)$ and $\mathcal{G}''(\omega_0)$ for intermediate monomer concentrations of 4μM with ATP regeneration system including Creatine Phosphate (CP) and Creatine Kinase (CK). Both measurements show the same behavior, i.e. the overshoot does not derive from lack of ATP.

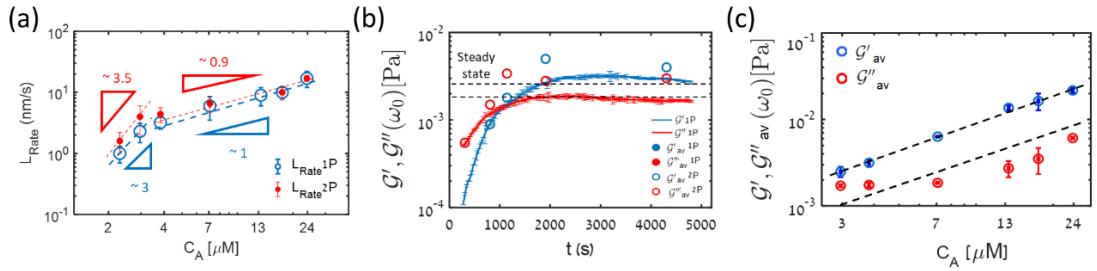

Fig. S5 Comparison between 1P and 2P microrheology of the kinetics of ATP-assisted self-assembly. (a) A comparison of the initial elongation rate L_{rate} extracted by 1P and 2P microrheology. Clearly, both methods agree well, demonstrating two regimes of concentration dependence. (b) Time evolution of $\mathcal{G}'(\omega_0)$ and $\mathcal{G}''(\omega_0)$ for monomer concentrations varying from 4μM as obtained from 1P and 2P microrheology calculations. The overshoot in $\mathcal{G}'$ is clearly seen in both cases. Dashed lines indicate the values of $\mathcal{G}'$, $\mathcal{G}''$ at steady state. (c) The value of $\mathcal{G}'$, $\mathcal{G}''$ at steady state are those obtained by averaging the value obtained for time windows larger than 3000 s in which the system arrives close to steady state.

C_A (μM)	c_a (mg/ml)	ξ (nm)	l_e (nm)	dt (nm)	τ_e (s)	ω_e (Hz)	ω_e (measured) (Hz)	τ_{rep} (s) 2P	τ_{rep} (s) 1P	ω_{rep} (mHz) 2P	L_{2P} (nm)	L_{1P} (nm)	t_{onset} (s)
2.37	0.10	950	1691	534	0.557	1.8	0.3	1704	21	0.6	13120	3050	---
2.97	0.12	850	1547	467	0.398	2.5	0.9	206	21	5	6257	2900	2200
3.81	0.16	750	1400	402	0.273	3.7	0.6	41	17	25	3500	2606	1161
7.08	0.30	550	1092	277	0.108	9.3	---	51	12	20	3400	2100	420
13.39	0.56	400	847	189	0.042	24.0	---	17	17	60	2100	2100	203
17.49	0.73	350	761	161	0.028	35.8	---	28	28	31	2500	2500	190
23.81	1.00	300	673	134	0.018	56.5	---	33	33	30	2400	2400	175

Table S1. Theoretical approximated steady state values according to Eq. (3) and [63]. It is important to note that the calculated final lengths in all concentrations except for 2μM are estimated and relative only since the model of diffusing rigid rods does not reliable for entangled networks.
Apparently, only at low actin monomer concentrations τ_{rep} is high enough to reach frequency window (e) in Fig.7 in the main text.

t(s)	Window in Fig.1	C_A (μM)	$C_{polymerized}$(t) (μM)	l_e(t) (nm)	dt(t) (nm)	τ_e (s)	ω_e (Hz)	ω_e (measured) (Hz)	τ_{rep} (s) 2P	ω_{rep} (mHz) 2P	L_{2P}(t) (nm)
150	(b)	2.97	0.203	4520	---	---	---	---	---	---	429
150	(c)	17.49	16.09	787	169	0.032	31.6	---	24	42	2300
210	(d)	17.49	16.30	783	168	0.031	32.1	---	25	40	2330
3600	(e)	2.97	0.963	1547	467	0.398	2.5	0.6	206	5	6252

Table S2. Theoretical approximated values related to Fig.1. Reptation time increases with window number (b-e) as expected. It is important to note that the calculated temporal lengths in 17μM at 210s and 3μM at 3600s are estimated and relative only since the model of diffusing rigid rods does not reliable for entangled networks.
The values for τ_e, ω_e, τ_{rep} and ω_{rep} cannot be calculated for C_A = 3μM (window (b)) since $l_e > L_{2P}(t)$.